To cite this version :

Laure ARBENZ, Abdelkader BENABOU, Stephane CLENET, Pierre FAVEROLLE, Jean-Claude MIPO - Characterization of the local incremental permeability of a ferromagnetic plate based on a four needles technique - IEEE Transactions on Magnetics - Vol. 53, n°3, p.1-7 - 2016

Characterization of the local incremental permeability of a ferromagnetic plate based on a four needles technique

Laure Arbenz[1,2], Abdelkader Benabou[1], Stéphane Clénet[1], Jean-Claude Mipo[2] and Pierre Faverolle[2]

[1] Univ. Lille, Centrale Lille, Arts et Métiers Paris Tech, HEI, EA 2697 - L2EP -Laboratoire d'Electrotechnique et d'Electronique de Puissance, F-59000 Lille, France
[2]Valeo – 94000 Créteil, France

The performances of electrical machines depend highly on the behavior of ferromagnetic materials. In some applications, these materials operate under DC polarization, i.e. when the magnetic field oscillates around a DC bias. In that condition, it is required to know the incremental permeability which characterizes the magnetic behavior of the material around the operating point. In this paper, a non-destructive approach, involving a combination of experiment and Finite Element (FE) technique, is presented in order to determine the incremental permeability. The proposed sensor is based on the four-needles method. With this sensor, Bowler et al. have proposed a method to determine the initial permeability of homogeneous metal plates based on an analytical model. Here we propose to use the same kind of sensor to determine the incremental permeability. The measurement process is analyzed using a FE model. It is shown that the analytical approach reaches its limits if the permeability of the plate and its thickness become too high. A combination between the measurements and a FE model is introduced to overcome this difficulty to determine the incremental permeability. The study of two magnetic steel samples illustrates the interest of this method.

Index Terms—Finite Element modeling, Four needles probe, Incremental permeability, Material characterization

I. INTRODUCTION

THE performance of an energy conversion device made up of ferromagnetic materials is highly dependent on their magnetic and electrical properties. The material behavior has to be characterized and modeled in order to study and predict the performance of the energy conversion device. To that end, the normal magnetization curve is usually used to represent the material behavior. Nevertheless, for some devices, such as the rotor of synchronous machine, the material is polarized and, in some regions of the rotor, the magnetic field can oscillate around a mean value. Therefore, the relevant magnetic characteristic is the incremental permeability that also depends on the magnetization level.

In the standard experimental approaches for magnetic measurement (Epstein frame, Single Sheet Tester), the characterization techniques require samples with a specific and simple geometry (steel sheet with standardized dimensions). This characterization is often carried out on the raw material before any manufacturing process. But an important aspect for the performance of the ferromagnetic pieces is related to the manufacturing process of the magnetic core that can modify the properties of the material. In fact, these can be worsened compared to the raw material [1]. Moreover, during the manufacturing process, this impact is not necessarily repetitive and can also lead to a dispersion of these properties. Characterization at the end of the process is sometimes preferable in order to identify the real behavior of the material. Therefore, a method of characterization, that must be non-destructive and local, is required.

The simple and obvious nondestructive approach consists in using a ferromagnetic yoke surrounded by an excitation coil. The magnetic field can be measured by a Hall sensor and the induction by a pick-up coil [2]. This method is largely used for nondestructive measurement and control in industry [3]. But this approach has some drawbacks. The main one is caused by the inevitably existing air gap between the yoke and the sample. Because this air gap cannot generally be controlled and is not necessarily the same from one sample to another, it is difficult to consider this method as quantitative.

Another interesting approach based on a four-point measuring sensor, known as ACPD (Alternating Current Potential Drop), is proposed in [4]. The ACPD method was historically developed as nondestructive testing since many years [5][6]. Bowler et al. have proposed to use this approach to measure the initial permeability quantitatively.

In this paper, and starting from the ACPD method, a quantitative method is developed in order to measure locally the incremental permeability of a ferromagnetic material up to saturation. A non-destructive approach, combining the experiment and the Finite Element (FE) technique, is proposed to extend the range of validity of the method. For the FE simulations, the 3D electromagnetic field calculation software *code_Carmel* is used [7].

First, the experimental method is detailed with the model used to identify the incremental permeability. Then, the proposed method is validated and used to characterize two kinds of magnetic steel plates.

II. EXPERIMENTAL PROCEDURE

A. Definition

The major (or main) hysteresis loop is the loop for which the material is magnetized up to saturation. Conversely, a minor loop is a loop for which the material is not magnetized to saturation. In Fig. 1., the major hysteresis loop and two minor loops are shown. The normal B(H) curve is obtained by connecting the tips (H_{max}, B_{max}) of minor loops with increasing values of H_{max}. Experimentally, this curve is similar to the

initial magnetization curve (or commutation curve). This latter is obtained when, from the demagnetized state, a strictly increasing field is applied [8].
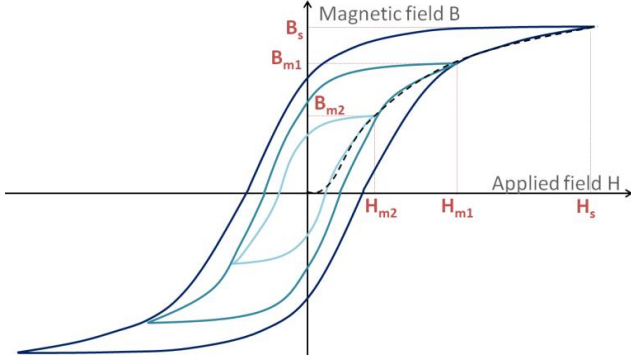

Fig. 1. Major hysteresis loop, minor loops and normal curve

If the material is initially demagnetized, a special case of minor loops is defined when the magnetization field is extremely small. Indeed, under these conditions, the magnetic behavior is in the Rayleigh region and the permeability is the initial permeability:

$$\mu_i= \lim_{(H\to 0)} \Delta B/\Delta H \qquad (1)$$

Note that, to perform a rigorous demagnetization of a material, this one has to be heated to a temperature above its Curie temperature. Then, the material is cooled in the absence of any external magnetic field. It is well known that, starting from this magnetic state, if an increasing magnetic field is applied, the obtained magnetization curve is known as the "virgin curve". In our case, a commonly used procedure is applied to obtain a magnetic state close to the demagnetization one. It consists in applying an alternating field with a magnitude high enough to cause the saturation of the material followed by a slowly decreasing magnitude to zero.

The initial permeability μ_i is therefore graphically represented by the slope of the initial minor loop (Fig. 2). The normal permeability μ_N is the slope of the normal curve. The incremental permeability μ_Δ is the slope of minor loops superimposed at various levels of biasing magnetic field (Fig. 2). For a given magnetic field, the normal and incremental permeability are different.
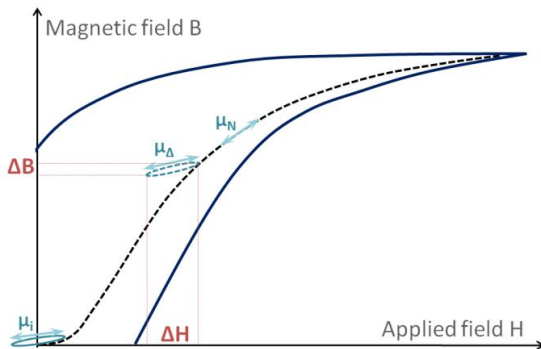

Fig. 2. Initial, Incremental and Normal permeability
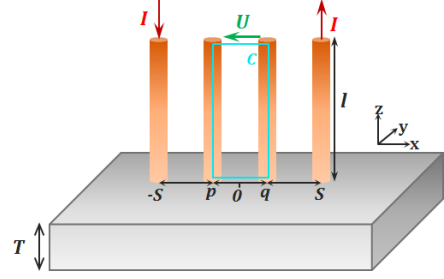
B. Presentation of the sensor

Fig. 3. Four-point device

For the experimental part, the developed sensor is based on the principle of the four-point method proposed by Valdes in 1954 [9]. In a previous work this approach was used to measure the electrical conductivity of electrical parts with a non-trivial geometry [10]. To measure the electrical conductivity, a DC current is imposed between the outer pair of points and a voltage is measured between the inner points (Fig.3). But, to measure the magnetic permeability, it is necessary to impose an AC current through the outer pair of points.

This measurement method, named four-point alternating-current potential drop (ACPD) method, has been studied in the case of ferromagnetic plates by Bowler et al. [4], [11]. The authors were interested in the case of homogeneous metal plates of which they proposed an analytical model to determine, from the experiment, the conductivity and the initial permeability of the plate. The voltage U is linked to the current I by the following expression:

$$U = \frac{I}{\pi}\left[-\frac{1}{\sigma T} + i\omega\mu_0\left(\frac{\mu_{ir}T}{3}+l\right) - \frac{\omega^2(\mu_0\mu_{ir})^2\sigma T^3}{45}\right] ln\left|\frac{1+q/s}{1-q/s}\right|, \text{f}<\text{f}_v \qquad (2)$$

With ω the angular frequency, σ the conductivity, $\mu_i=\mu_{ir}\mu_0$ the initial permeability, parameters T, l, q, s defined in Fig.3 and Fig.4 and $f_v= \pi/(2\mu_i\sigma T^2)$. Indeed, from this expression, the conductivity σ (or the thickness T) and the initial permeability μ_i can be determined from the measurements of the real and imaginary parts of the voltage U. Nevertheless, this approach allows measuring only the initial permeability μ_i. To obtain the incremental permeability μ_Δ versus the polarization field H_{pol}, it is necessary to add to the four-point sensor a polarization device and a field sensor.

C. Experimental device

A ferromagnetic yoke ($30\times40\text{mm}^2$ of section for a height of 130 mm and a length of 150 mm), carrying a bias coil (200 turns, 0.6 mm wire diameter), is added to the experimental device to create the polarization magnetic field H_{pol} in the sample. The magnetic field at the surface of the sample can be estimated from a measurement with a Hall sensor. But, the magnetic field gradient in the air gap between the Hall sensor and the surface of the sample can lead to significant measurement errors. So, a more accurate technique consists in using a probe made with two Hall sensors (Allegro MicroSystems Inc A1389LLHLX-9-T), superposed one on the

other below the sample. The magnetic field H_1 (respectively H_2) is measured by the Hall sensor at the distance z_1 (respectively z_2) from the sample surface. Then, the surface magnetic field H_{pol} is obtained directly by a linear extrapolation. Indeed, H_{pol} is the intercept point of the linear function as $z(H_{pol})=0$, so:

$$H_{pol} = (z_2 H_1 - z_1 H_2) / (z_2 - z_1) \qquad (3)$$

The probe is placed next to the four-point sensor to measure the field and the voltage at the same location (Fig.4). The four-point sensor is made with four spring loaded needles of 1mm diameter (Ingun HSS118) with round tip style to ensure a good point contact and gold plating.
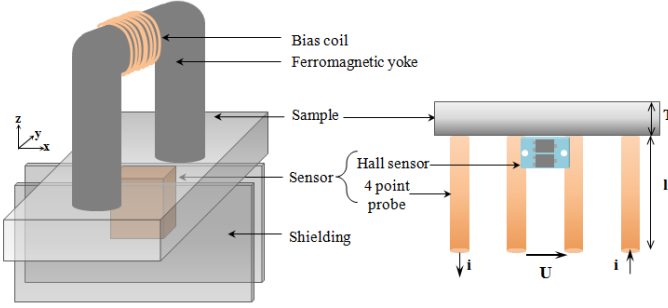

Fig. 4. Proposed experimental device

Moreover, a magnetic shield is added to reduce the magnetic field gradient in the vicinity of the Hall sensors. This allows a better estimation, from equation (3), of the magnetic field at the surface of the sample. The shielding is made of two magnetically soft steel sheets.

D. Raw measurement interpretation

In practice, considering the alternating excitation current i in the outer points as the phase reference, the measured voltage U between the inner points (see Fig. 3) is post-processed in order to extract its real and imaginary parts (U_r and U_i). To do so, the RMS values (i_{eff} and U_{eff}) and the average power P are calculated:

$$i_{eff} = \sqrt{\frac{1}{T_p} \int_{t_0}^{t_0+T_p} i^2(t)dt}, \qquad U_{eff} = \sqrt{\frac{1}{T_p} \int_{t_0}^{t_0+T_p} U^2(t)dt},$$

$$P = \frac{1}{T_p} \int_{t_0}^{t_0+T_p} i(t)U(t)dt \qquad (4)$$

with t_0 a time instant arbitrary chosen and T_p the period of the excitation signal. The integration is performed numerically by applying the trapezoidal rule. From the result of equation (4), the phase lag between the current and the voltage is deduced by:

$$\cos\varphi = P/(i_{eff}\, U_{eff}) \quad \text{and} \quad U_{amp} = U_{eff}\, \sqrt{2} \qquad (5)$$

Then one can easily determine the real and imaginary parts of the signal by:

$$U_r = U_{amp}\, \cos\varphi \quad \text{and} \quad U_i = U_{amp}\, \sin\varphi \qquad (6)$$

To summarize, the polarization field H_{pol} is directly measured with the field sensor (see Fig.4). The incremental permeability μ_Δ must be deduced from the real and/or imaginary parts of the voltage (U_r and U_i) using an analytical or numerical model. Indeed, equation (2) can be used replacing μ_{ir} by $\mu_{\Delta r}$. We assume that the hysteresis loop of interest is just shifted on the first magnetization curve. As mentioned previously (see equation (2)), the analytical model proposed by Bowler *et al.* having a limited range of application, we propose to perform the extrapolation of the incremental permeability from a numerical model.

III. NUMERICAL MODELING

A. Presentation of the approach

For the analytical development proposed by Bowler et al., some hypotheses are necessary, such as constant permeability and far-field regime [8], [9]. Moreover, the obtained analytical model is valid if the frequency is less than $f_v = \pi/(2\mu\sigma T^2)$, with $\mu=\mu_i$ or μ_Δ corresponding to the skin effect limit. However, in practice this frequency limit can be quickly reached. For example, in the case of a 2 mm thick plate with electrical conductivity 5.5MS/m and relative permeability 800, the limit frequency is only 70 Hz. This limit frequency f_v reduces the experimental data available, which is limiting to identify with accuracy the permeability.

Therefore, we propose to use a FE model instead. The numerical model was built upon several hypotheses. The first one is the delimitation of the studied domain that includes the plate with the needles and an air box surrounding the device. This air box is chosen with its boundaries sufficiently far from the plate in order to allow the leakage magnetic flux to flow through the air. On the needles side, the air box boundary coincides with the top of the needles in order to impose the current, in the excitation needles, at the boundary of the studied domain. Regarding the needles, these have been idealized with a cylindrical shape so that the contact with the plate is a surface delimited by a circle. Also, the needles were considered with a conductivity equal to 60 MS/m. Another modelling hypothesis is the neglecting of the magnetic shield on the opposite side of the plate as it was verified experimentally that it does not influence the AC field produced by the excitation needles. As previously mentioned, its usefulness is relevant for the experimental estimation of the magnetic field at the surface of the plate. Finally, the simulated geometry consists in the sample (2mm x 50mm x 200mm), the four-point sensor and the air around the device (88mm x 250mm x 400mm) (Fig. 5).
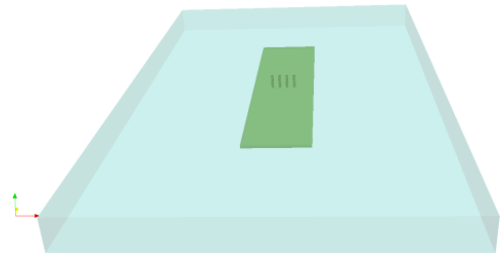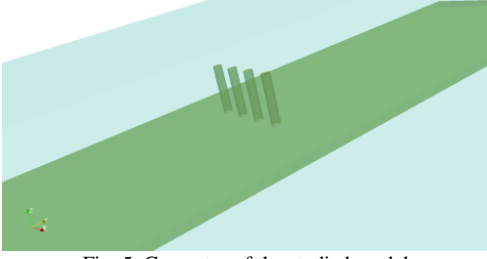
Fig. 5. Geometry of the studied model

The solution is obtained by solving a quasistatic problem using the electric potential (A-φ) formulation with the Finite Element Method. The quantities of interest are the voltages and the currents at the terminals of the needles under sinusoidal excitation and in steady state. Since the problem is linear, it has been solved in the frequency domain. To get accurate results, the global quantities have been either imposed or calculated in post-processing using a method presented in [12] which imposes a power balance (the mean of the eddy current losses is equal to the active power and the mean of the magnetic energy is equal to the reactive power provided by the external circuit). For a fixed thickness T and a fixed conductivity σ and different values of the relative permeability μ_r, the AC current flowing through the external needles of the sensor is imposed and the resulting voltage between the internal needles is calculated in a post-processing step for different frequencies. The discretization of the domain leads to a mesh of 250 000 nodes and 1 500 000 tetrahedral elements.

As illustration, some results are presented in Fig. 6 and Fig. 7 where the real and imaginary parts of the simulated signals are reported obtained with the FE model and the analytical expression (2). Since the FE model can be considered as the reference one, from these results, the limit of validity of the analytical approach appears clearly. Above a given frequency (close to f_v) the analytical and the numerical models are not in agreement anymore.
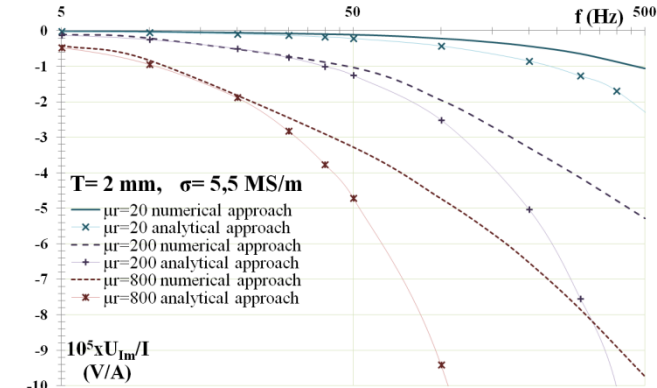

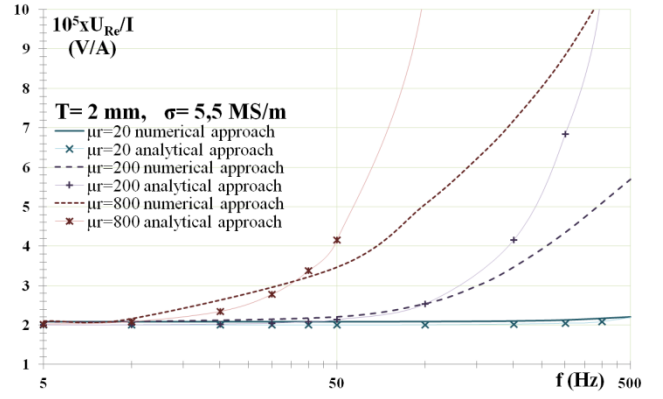Fig. 6. Imaginary voltage divided by imposed current versus frequency of the imposed current

Fig. 7. Real voltage divided by imposed current versus frequency of the imposed current

B. Current density and magnetic flux distribution

To further analyze the behavior of electromagnetic quantities in the plate, an example of current density distribution is given in Fig. 8. It is observed that the current is widely distributed in the plate.
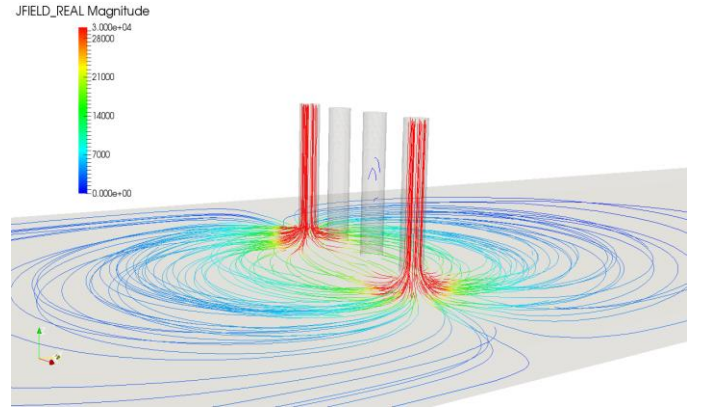

Fig. 8. Current density distribution (f= 5Hz, μr=5)

Fig. 9 shows the magnetic flux density component along the y axis, in the plane containing the four-point sensor. It is very interesting to notice that the magnetic flux flowing between the measurement points (i.e. inner points) is unidirectional (here, in the opposite direction of the y axis orientation). Indeed, the magnetic flux path closes outside of the sensor measurement region. Consequently, at the measurement points, the magnetic induction profile is quite simple.
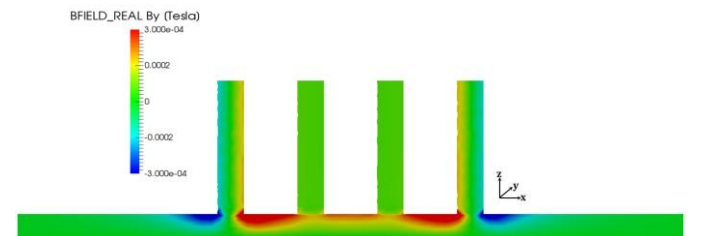

Fig. 9. Magnetic induction along the y axis (f= 5Hz, μr=5)

The Fig. 10 (f=5Hz) shows the magnetic induction component along the y axis for different cross-sections along the y axis. It is noted that, for the sample having an incremental permeability μ_r=5, the magnetic flux density is

not distributed in all the plate. In fact, the magnetic flux closes rapidly in the region outside the sensor. But, for the sample with a higher incremental permeability μr=800 (Fig.11, f=5Hz), the magnetic flux is distributed in all the plate and reaches greater distances before changing its direction. The end effect should be taken into account which is naturally done using the FE model but not with the analytical approach where the plate is assumed to be infinite.
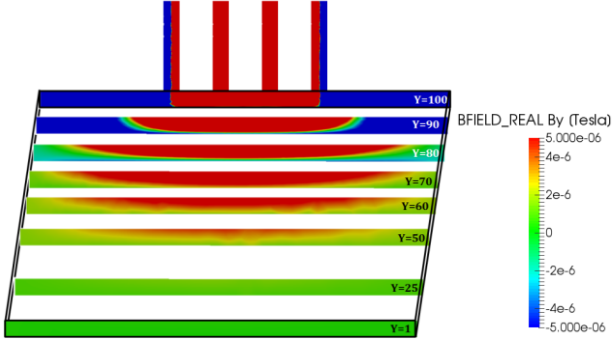

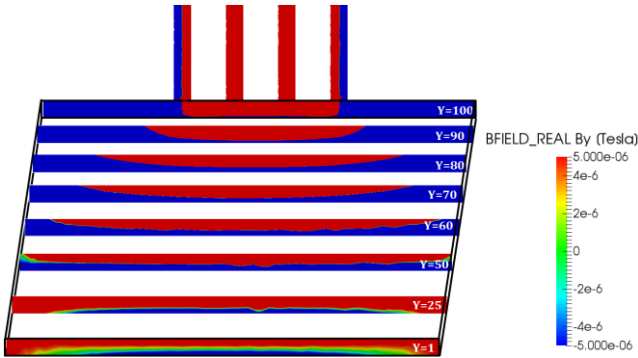Fig. 10. Magnetic induction along the *y* axis on all the sample (μr=5)

Fig. 11. Magnetic induction along the *y* axis on all the sample (μr=800)

C. Application to the measurement of the permeability

The FE simulations allow the extraction of the voltage response for several values of the incremental permeability μ_Δ. These results are used as an abacus for identifying the practical incremental permeability by a comparison with the measured voltage. To perform this operation, it is necessary to know the thickness and conductivity of the studied sample. Then, for fixed thickness (*T=2 mm*), fixed conductivity which can be measured with a DC method [10] (*σ=5,5MS/m)* and different values of the relative permeability μ_r, the numerical results are used to calculate the real and imaginary voltages (U_r and U_i) versus the frequency of the AC current flowing through the external needles of the sensor (Fig.12).
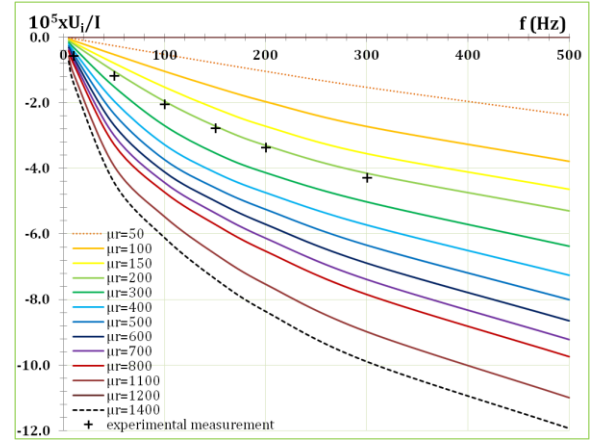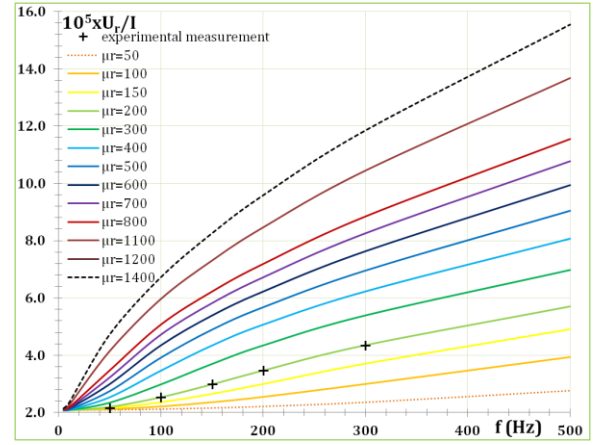

Fig. 12. Numerical results (T= 2 mm, σ=5,5 MS/m) with experimental measurements represented with +

The experimental results (real and/or imaginary parts) can be then plotted together with the numerical results in order to identify the closest incremental permeability. To ensure a robust identification, a frequency sweep is performed to find the best curve fit. In the example of Fig. 12, the deduced permeability in both cases (real and imaginary parts) is 200.

IV. VALIDATION OF THE MEASUREMENT METHOD

A. Sample description

The following study proposes to compare the incremental permeability of two samples of magnetic steel (SAE 1006). The aim is to validate the ability of the proposed method to quantitatively estimate the incremental permeability. Both studied samples have a thickness T=2 mm and a conductivity σ=5.5 MS/m. The conductivity of the material has been determined by the method presented in [10] which is based on four needle technic supplied by a DC voltage coupled with the FE model. From the same experimental device and FE model the conductivity and the incremental permeability can be determined. They have the same chemical composition but a different microstructure due to a different heat treatment. Indeed, the sample noted **B0** is raw and the sample note **B1** has been annealed.

Both of these samples were magnetically characterized by a single sheet tester (SST, Brockhaus measurements) at 1Hz. Normal curves of samples are deduced from a set of centered

minor loops (Fig. 13). The obtained normal curves show that the magnetic properties of both samples are indeed different: the annealed has improved the magnetic characteristics of sample **B1.**
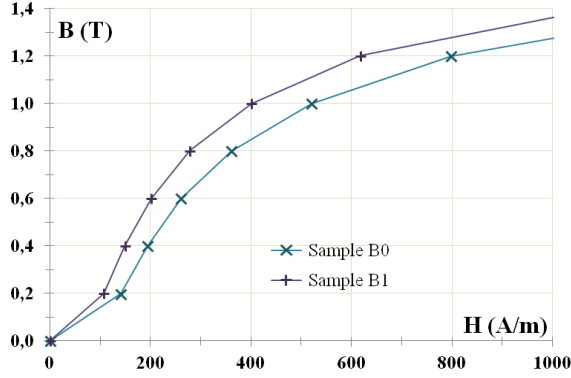

Fig. 13. Normal curves of the studied samples

B. Reference incremental permeability

Regarding the reference incremental permeability that will be used to validate the four needles technique, a graphical approach, using the minors loops measure using the SST device is adopted. In Fig. 14, we present the principle to determine the incremental permeability for a given value of the magnetic field H_{pol}. More precisely, for a given width ΔH, at the extremity of the minor loop, an interval of the magnetic induction ΔB is identified. Then, the ratio of these two values allows deducing the incremental permeability μ_Δ. In addition, the polarization field H_{pol} is assumed to be the center of the interval ΔH. This operation is reproduced for all minor loops and the curve $\mu_\Delta = f(H_{pol})$ is obtained. We can see that the value of the incremental permeability is dependent of the width ΔH. Consequently, the width of the incremental loop ΔH should be chosen to be of the same order of the one met with the four-point technic. In the four needles method this width ΔH is linked to the amplitude of the AC current imposed through the needles. So it is important to measure the corresponding ΔH in order to extract the correct reference incremental permeability from the minor loops.
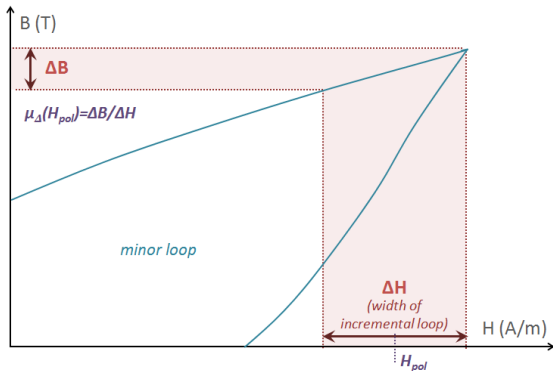

Fig. 14. Method to obtain the reference incremental permeability

In Fig. 15, we have represented the incremental permeability in function of H_{pol} for three values of ΔH determined from SST measurement and the method described above. The importance of the accurate knowledge of ΔH is illustrated, particularly for low polarization magnetic fields where an important dispersion is observed for the three tested ΔH values.
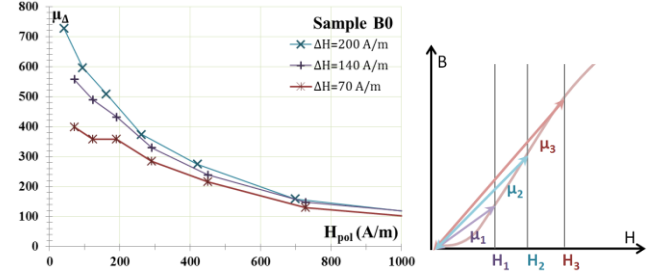

Fig. 15. Reference incremental permeability - effect of ΔH

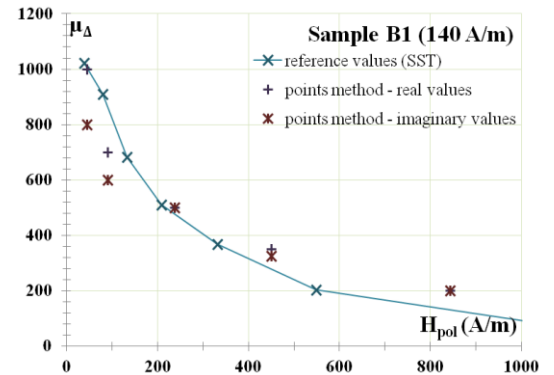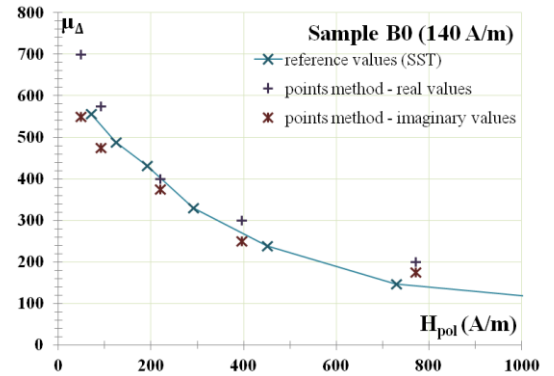### C. Validation of the proposed method

Fig. 16. Experimental results - comparison with reference values

The approach of incremental permeability identification is then applied to the samples **B0** and **B1**. The experimental results are given in Fig. 16 where the real and imaginary values represent the results of the identification procedure performed with the simulated curves of, respectively, the real and imaginary parts of the voltage. We can notice that experimental results obtained from both real and imaginary parts are close. Moreover the measured data are also close to the reference values.

We can see that this method enable to it is possible to distinguish the samples from each other with the proposed method.

V. Conclusion

The proposed approach enables to deduce the magnetic characteristics of steel plates without extracting specific samples. The procedure was applied to steel plates with the same thickness and composition but with different magnetic characteristics. The results show that the studied samples exhibit different incremental permeability which evolution versus the polarization field, being clearly different, allows to distinguish the magnetic steels.

This study shows also that the behavior of the incremental permeability is complex as it depends on the width of the minor loop and considered material. This method is attractive as it is easy and fast to carry out experimentally. Moreover, using the combined experimental-numerical approach, the method can be easily applied to more complex geometries in a non-destructive context.

References

[1] R. Ramarotafika, A. Benabou, S. Clenet, J-C. Mipo, "Experimental Characterization of the Iron Losses Variability in Stators of Electrical Machines", *IEEE Trans. Magn.*, vol. 48, no. 4, pp. 1629-1632, 2012.

[2] O. Stupakov, H. Kikuchi, T. Liu et T. Takagi, "Applicability of local magnetic measurements" Measurement, vol. 42, n°15, pp. 706-710, 2009

[3] Y. Gabi, B. Wolter, A. Gerbershagen, M. Ewen, P.Braun, O. Martins "FEM Simulations of Incremental Permeability Signals of a Multi-Layer Steel With Consideration of the Hysteretic Behavior of Each Layer" *IEEE Trans. Magn.,* vol.50, no. 4, 2014.

[4] N. Bowler, "Four-point potential drop measurements for materials characterization", *Meas. Sci. Technol., vol. 22, 2011*

[5] D.H. Michael, R.T. Weachter, R. Collins, "The Measurement of Surface Cracks in Metals by Using a.c. Electric Fields ", *Proc. R. Soc. Lond. A,* vol. 381, No. 1780, pp. 139-157, 1982

[6] D.H. Michael, R. Collins, W.D. Dover " Detection and Measurement of Cracks in Threaded Bolts with an a.c. Potential Difference Method", *Proc. R. Soc. Lond. A,* vol. 385, No. 1788, pp. 145-168, 1983

[7] code_Carmel (Code Avancé de Recherche en Modélisation Electromagnétique), L2EP, University of Lille1, http://code-carmel.univ-lille1.fr

[8] R. M. Bozorth, "Ferromagnetism", IEEE Press, p3-7, 1993.

[9] B. Valdes, "Resistivity measurements on germanium for transistors", *Proceedings of the I. R. E*., vol. 42, pp. 420-427, 1954.

[10] L. Arbenz, A. Benabou, S. Clénet, J.-C. Mipo, P. Faverolle, "Characterization if the local electrical properties of electrical machine parts with non -trivial geometry", *Int. J. Appl. Electrom*., vol. 48, p201-206, 2015

[11] N. Bowler, Y. Huang, " Model-Based Characterization of Homogeneous Metal Plates by Four-Point Alternating Current Potential Drop Measurements", *IEEE Trans. Magn,* vol.41, no. 6, pp. 2102-2110, 2005.

[12] T. Henneron, S. Clénet, F. Piriou, "Calculation of Extra Copper Losses with Imposed Current Magnetodynamic Formulations", *IEEE Trans. Magn*., vol. 42 ,no. 2, pp 767-780, 2006